

AD706120



RRA RADIATION RESEARCH ASSOCIATES
Fort Worth, Texas 76107

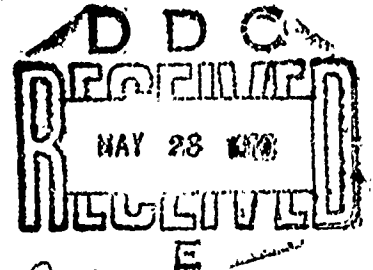
**FLASH, A MONTE CARLO PROCEDURE
FOR USE IN CALCULATING LIGHT SCATTERING
IN A SPHERICAL SHELL ATMOSPHERE**

by
Dave G. Collins and Michael B. Wells

Contract No. F19628-67-C-0298
Project No. 7621
Task No. 762107
Work Unit No. 76210701

Final Report
1 May 1967 — 31 January 1970
31 January 1970

Contract Monitor
Frederic E. Volz
Optical Physics Laboratory



This document has been approved for public
release and sale; its distribution is unlimited.

Reproduced by the
CLEARINGHOUSE
for Federal Scientific & Technical
Information Springfield Va 22151

Prepared for
AIR FORCE CAMBRIDGE RESEARCH LABORATORIES
OFFICE OF AEROSPACE RESEARCH
UNITED STATES AIR FORCE
Bedford, Massachusetts 01730

AFCRL-70-0206

RRA-T704

FLASH, A MONTE CARLO PROCEDURE FOR USE
IN CALCULATING LIGHT SCATTERING IN A
SPHERICAL SHELL ATMOSPHERE

by

Dave G. Collins and Michael B. Wells

Radiation Research Associates, Inc.
3550 Hulen Street
Fort Worth, Texas 76107

Contract No. F19628-67-C-0298
Project No. 7621
Task No. 762107
Work Unit No. 76210701

Final Report
1 May 1967-31 January 1970
31 January 1970

Contract Monitor-
Frederic E. Volz
Optical Physics Laboratory

This document has been approved for public
release and sale; its distribution is unlimited.

Prepared for
Air Force Cambridge Research Laboratories
Office of Aerospace Research
United States Air Force
Bedford, Massachusetts 01730

ABSTRACT

A program designated FLASH has been developed to provide a means to study the propagation of monochromatic radiation from a plane parallel source through a spherical shell atmosphere.

A simple illustration of the backward Monte Carlo method utilized in the development of the FLASH program is discussed in order to show the advantage of the method.

A brief description of the methods employed in the FLASH program is given to illustrate the application of the backward Monte Carlo treatment of light propagation through a spherical shell atmosphere.

Several comparisons of FLASH generated data with data from other calculational methods are shown.

TABLE OF CONTENTS

<u>Title</u>	<u>Page</u>
ABSTRACT	iii
LIST OF FIGURES	vii
LIST OF TABLES	ix
I. INTRODUCTION	1
II. MONTE CARLO METHOD	3
2.1 Backward Monte Carlo	4
2.2 Illustration of Backward Monte Carlo	6
III. CALCULATIONAL METHODS FOR SCATTERED LIGHT	10
3.1 Polarization Parameters	10
3.2 Problem Geometry	11
3.3 Selection of Receiver View Angles	13
3.4 Distance to Collision	15
3.5 CO ₂ and Water Vapor Absorption	16
3.6 Direction Before Collision	18
3.7 Effects of Changes in Index of Refraction	20
3.8 Selection of the Scattering Event	20
3.9 Selection of Direction to Source	21
3.10 Polarization Parameter After Scattering	23
3.11 Estimate of the Scattered Intensity	25
3.12 Selection of Direction to Previous Collision	25
3.13 Ground and Cloud Reflection	27

TABLE OF CONTENTS (Continued)

<u>Title</u>	<u>Page</u>
IV. FLASH CALCULATIONS	29
4.1 Comparisons for Rayleigh Scattering	29
4.2 Comparisons for Aerosol Scattering	33
4.3 Intensity Emerging from Earth's Atmosphere	35
4.4 Twilight Studies	39
V. REFERENCES	45

LIST OF FIGURES

<u>Figure</u>	<u>Page</u>
1. Geometry for Plane Parallel Source and Receiver Embedded within an Infinite Media.	9
2. Receiver View Angles	14
3. Displacement Angles	19
4. Geometry for Calculation of Scattering Angle Between Direction to Source Plane and Direction Before Collision	22
5. Intensity Transmitted Through A Rayleigh Atmosphere of Optical Thickness Equal to 1; Plane Source Incident at Arccosine = 0.92.	31
6. Intensity Transmitted Through A Rayleigh Atmosphere of Optical Thickness Equal to 1; Plane Parallel Source Incident at Arccosine = 0.4.	32
7. Distribution with Altitude of the Aerosol Attenuation Coefficient for 0.55 Micron Wavelength Light in the Hazy Atmosphere.	34
8. Comparison of Data From A RRA-89 Calculation with Data From a FLASH Calculation for a Wavelength of 0.37 μ .	37
9. Comparison of Data From A RRA-89 Calculation with Data From a FLASH Calculation for a Wavelength of 0.78 μ .	38
10. Aerosol Attenuation Profiles Used in Twilight Studies.	40
11. Scattered Light Intensity at 20 Degrees Elevation Versus Sun Depression Angle for Aerosol Profile A: 0.7 μ Wavelength Light.	42

LIST OF FIGURES (Continued)

<u>Title</u>	<u>Page</u>
12. Scattered Light Intensity at 20 Degrees Elevation Versus Sun Depression Angle for Aerosol Profile C: 0.7μ Wavelength Light.	43
13. Single Scattered Intensity for a Sun Depression Angle of 0° as a Function of Altitude in Atmospheres A and C: $\lambda = 0.7\mu$.	44

LIST OF TABLES

<u>Table</u>	<u>Page</u>
I. Comparison of Scattered Light Intensity Transmitted Through Spherical and Plane Rayleigh Atmospheres of a Unit Optical Thickness.	30
II. Comparison of Scattered Light at 10 Kilometers Altitude in a Haze Atmosphere From Plane and Spherical Geometry Calculations.	36

I. INTRODUCTION

During the contract period, 1 May 1967 to 31 January 1970, work was performed on five major work areas. These areas include: (1) the development of the LITE-II Monte Carlo procedure for study of sunlight, moonlight, and night light transport in a plane parallel atmosphere and the application of the LITE-II Monte Carlo procedure to calculations for two model atmospheres; (2) the development of the LITE-I Monte Carlo procedure for study of atmospheric transport of light emitted by point monodirectional sources and the application of the LITE-I Monte Carlo procedure to the analysis of measured searchlight scattering data; (3) the application of the LITE-I Monte Carlo procedure to the study of laser radiation backscattering from the ground surface and the scattering of laser radiation by the atmosphere; (4) an analysis of the computer calculations performed under Item 1 to give contrast transmission data for the two model atmospheres considered; and (5) the development of the FLASH Monte Carlo procedure to treat sunlight transport in a spherical geometry atmosphere and the application of the FLASH procedure to determine skylight distributions for twilight scattering problems.

The work performed under Items 1 through 4 above have been previously reported in References 1 through 7. This report describes the work performed for Item 5.

Most previous calculational methods developed to analyze the propagation of sunlight within the earth's atmosphere have utilized plane parallel atmospheric geometries, Ref. 8 - 12. The plane parallel geometry, however, does not adequately represent the earth's atmosphere for twilight conditions.

In an effort to provide a calculational tool to compute the radiation intensity at twilight, a Monte Carlo program has been developed to treat

the propagation of visible and infrared radiation through a spherical shell atmosphere. The program, designated as FLASH, utilizes the backward Monte Carlo approach to compute the scattered light intensity from sunlight as a function of view angle for receivers located within or above the earth's atmosphere. The Monte Carlo method was selected because of the need to evaluate the contributions from multiple scattering and because of the versatility offered in its application to complex geometries. The FLASH program also takes into account the bending of the sun rays (photon paths) by the change in the atmospheric index of refraction with altitude.

1.1. MONTE CARLO METHOD

In the application of the Monte Carlo method to obtain the solution to an integral such as

$$\int_a^b f(x) dx,$$

the common practice is to express $f(x)$ as the product of two functions, $h(x)$, a density function, and $g(x)$, an estimating function. To evaluate the integral

$$\int_a^b h(x) g(x) dx,$$

the density function is normalized by multiplying by a constant, c , where c is given by

$$c \int_a^b h(x) dx = 1$$

A random value of x is sampled from the normalized density function by evaluating the equation

$$RN = \int_a^{x_1} ch(x) dx,$$

where $a \leq x_1 \leq b$ and RN is a random number drawn from a uniform distribution between 0 and 1. An estimate of the integral

$$\int_a^b f(x) dx$$

is obtained by averaging the estimator function

$$\text{EST} = g(x_i) / c$$

for the sample values x_i . An average of $g(x_i)/c$ for a large number, N , of random values of x_i as given by

$$\frac{1}{N} \sum_{i=1}^N g(x_i) / c$$

is an estimate of the mean value of the integral.

An arbitrary division of $f(x)$ into density and estimating functions may result in an estimating function that produces extremely high values of $g(x)/c$ for some of the values of x sampled from the density function. In selecting the estimating function, the objective should be to obtain a function that remains within reasonable limits for all of the sampled values. The portion of the integrand selected as the density function should be a function from which it is easy to obtain sample values. In some cases, a better separation of the integrand into density and estimating functions can be achieved if the integral expression can be rewritten with a change of variables.

2.1 Backward Monte Carlo

When using the Backward Monte Carlo approach to calculate the scattered light intensity at a point receiver due to a plane parallel source incident upon a spherical shell atmosphere, a change in variables in the integral form of the transport equation yields an integrand which is expressed in terms of integration variables defined about the receiver position rather than about the source position.

It will be shown that the integral expressed in terms of variables defined with respect to the receiver position allows the selection of an estimating function that has less variation with random values sampled from the density function than that which would be obtained when the variables of integration are expressed in terms of the source position.

A physical interpretation of the Monte Carlo solution of the integral expressed in terms of variables defined about the receiver is that photon histories are started at the receiver and traced backward to the source position.

The backward approach is particularly advantageous for those problems in which the scattered intensity at the receiver is desired for only a portion of the total solid angle. The backward approach, in this case, will allow all samples to be taken within the solid angle of interest. For a plane source, the backward approach provides an optimum sampling of the areas on the source plane that have the greatest possibility of contributing to the scattered intensity at the receiver position.

Care must be exercised in the application of backward Monte Carlo (starting particle histories at the receiver and estimating the direct intensity at the first collision) to insure that the integral equation solved is equivalent to the actual physical situation. The approach taken was to write the integral equation which represents a direct interpretation of the single scattered intensity and then to change the variables of integration so that sampling of the particles random path may be started at the receiver position. If the limits of integration on the forward form of the scattering integral are transposed in accordance with the change of variables for the backward calculation, the resulting equation should not only yield the same results as the original equation, but it should lend itself to a more economical solution.

2.2 Illustration of Backward Monte Carlo

For illustration, consider an infinite plane parallel source embedded within an infinite media which scatters radiation isotropically. Suppose that one wishes to know the average single scattered intensity at some distance Z_0 from the source plane, Figure 1. The expression for the single scattered intensity may be written as follows,

$$SI = \int_0^{2\pi} \int_0^{\infty} \int_0^{\infty} S(\rho, \phi) \Sigma_T e^{-\Sigma_T Z} (1/4\pi) \frac{e^{-\Sigma_T r}}{r^2} \rho d\rho d\phi dZ \quad (2.1)$$

where $S(\rho, \phi)$ is the source strength at the position ρ, ϕ on the source plane, Σ_T is the extinction coefficient of the media, Z is the distance from the source plane to the collision point, and r is the distance from the collision to the receiver position. Equation 2.1 could be solved with the Monte Carlo method or some other method of numerical integration, but some decision must be made as to what the upper limit of the integral over the source radius will be and what delta ρ values will yield the most efficient calculation. This is especially true of a Monte Carlo solution of Equation 2.1, because if one should select the position of the source photon from a uniform distribution over some finite portion of the plane, he could easily be concentrating his sampling at large radial distances that produce no significant single scattered intensity at the receiver position.

A better method for solving Equation 2.1 would be to change the variables of integration from ρ and Z to Θ and r , where the relationship between the variables are as follows:

$$\begin{aligned} \rho &= r \sin\Theta \\ Z &= Z_0 - r \cos\Theta . \end{aligned}$$

Since ρ and Z are both functions of r and θ , we may transform Equation 2.1 into an equation expressed in terms of r and θ through the use of the following relation:

$$\iint f(\rho, Z) d\rho dZ = \iint f(\rho(r, \theta), Z(r, \theta)) \left| \frac{\partial(\rho, Z)}{\partial(r, \theta)} \right| dr d\theta$$

where $\left| \frac{\partial(\rho, Z)}{\partial(r, \theta)} \right|$ is the absolute value of the Jacobian.

Solving for the partial derivative in the Jacobian we obtain:

$$\frac{\partial \rho}{\partial r} = \sin \theta$$

$$\frac{\partial \rho}{\partial \theta} = r \cos \theta$$

$$\frac{\partial Z}{\partial r} = -\cos \theta$$

and

$$\frac{\partial Z}{\partial \theta} = r \sin \theta .$$

Evaluating the Jacobian yields

$$\begin{vmatrix} \frac{\partial \rho}{\partial r} & \frac{\partial \rho}{\partial \theta} \\ \frac{\partial Z}{\partial r} & \frac{\partial Z}{\partial \theta} \end{vmatrix} = r .$$

Rewriting Equation 2.1 by substituting r and θ for ρ and Z gives:

$$SI = \int_0^{2\pi} \int_0^{\infty} \int_0^{\pi} S(\rho, \phi) * e^{-\Sigma_T(Z_0 - r \cos \theta)} (1/4\pi) e^{-\Sigma_T r} \sin \theta d\theta dr d\phi \quad (2.2)$$

Equation 2.2 may be solved using the Monte Carlo method by sampling a value of θ from $\sin \theta d\theta/2$, a value of θ from $d\theta/2\pi$ and a value of r from

$\Sigma_T e^{-\Sigma_T r}$ dr and evaluating the remainder of the expression under the integral

$$S(\rho(r, \theta), \phi) e^{-\Sigma_T(Z_0 - r \cos \theta)}$$

for the values sampled for r, θ , and ϕ .

Note that the integration of θ in Equation 2.2 is over a finite range and since the integral of

$$\Sigma_T e^{-\Sigma_T r} dr$$

has a value of one when integrated from 0 to infinity, values of r approaching infinity may be selected and thus values of $\rho = r \sin \theta$ are also unlimited.

Note also that the density function

$$\Sigma_T e^{-\Sigma_T r}$$

and the estimating function

$$e^{-\Sigma_T(Z_0 - r \cos \theta)}$$

both peak for small values of r indicating the sampling is concentrated near the area where the estimating function has its highest value. A situation of this nature produces less statistical fluctuation than would be expected for a Monte Carlo solution of Equation 2.1.

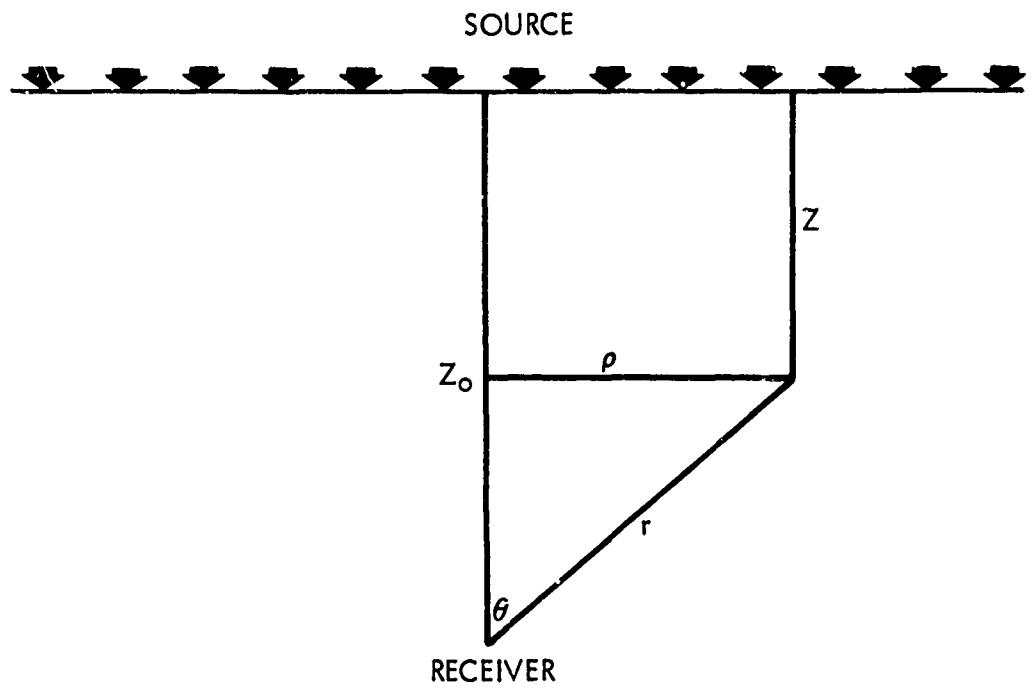


Fig. 1. Geometry for Plane Parallel Source and Receiver Embedded within an Infinite Media

III. CALCULATIONAL METHODS FOR SCATTERED LIGHT

The backward Monte Carlo method discussed in Section II has been utilized in the development of the FLASH program to provide a means to study the transport of visible and infrared radiation within a spherical shell atmosphere. A pure mathematician would probably be satisfied with a presentation of the methods utilized in FLASH as a method of numerically integrating the integral form of the transport equation. He would not necessarily require a physical interpretation of the method. Others, however, conceive of the Monte Carlo approach as an experiment performed on a digital computer where the sampling schemes are related to the probability distributions of the possible events that may occur in tracing a quantum of energy as it scatters through the atmosphere. Applying this concept to the solution of the transport equation expressed in terms of variables defined with respect to the receiver positions results in tracing the quantum of energy (photon) in a backward direction from the receiver to the source and thus the term backward Monte Carlo. While the concept of the photon going backward is physically unrealistic, it does provide a means of interpreting the detailed calculations that are performed by FLASH when solving the radiation transport equation.

3.1 Polarization Parameters

The initial intensity and polarization characteristics of the radiation at the receiver position are defined in terms of the polarization parameters I_{\perp} , I_{\parallel} , U and V which are related to the Stokes parameter I , Q , U , and V by the relations

$$I = I_{\perp} + I_{\parallel}$$

$$Q = I_{\perp} - I_{\parallel}$$

$$U = U$$

$$V = V$$

These parameters are defined with reference to a plane containing the radial through the receiver position and the direction of propagation of the light incident at the receiver. The sunlight incident upon the earth's atmosphere is considered to be unpolarized, therefore, the polarization parameters are initialized to

$$I_{\perp} = 0.5W$$

$$I_{\parallel} = 0.5W$$

$$U = 0.0$$

$$V = 0.0$$

where W is a weight parameter initially set equal to a unit intensity incident from the direction of propagation into the receiver position. Processes such as absorption that affect all polarization parameters in the same manner are included by an adjustment to the weight parameter while processes such as Rayleigh and aerosol scattering require individual adjustment of the polarization parameters. The product of the weight parameter times the sum of the first two polarization parameters gives the photon intensity at any position in the atmosphere. The degree of polarization at any position is given by

$$p = \frac{\left((I_{\perp} - I_{\parallel})^2 + U^2 + V^2 \right)^{1/2}}{(I_{\perp} + I_{\parallel})}$$

Since the atmospheric parameters which affect the transport of light all vary with altitude, it was necessary that the geometry of the FLASH program be capable of providing a means of defining the atmospheric conditions as a function of altitude.

3.2 Problem Geometry

The geometry portion of the FLASH program provides for the division of a spherical shell atmosphere into as many as 100 spherical shell layers or atmospheric layers. The spherical shell layers are defined

by inputting the altitudes of the spherical surfaces separating the layers. The atmospheric conditions at each boundary are defined by inputting the optical distance from ground level to the boundary altitude, the ratio of the scattering-to-pseudo extinction coefficient at the boundary altitude, the ratio of the Rayleigh-to-scattering coefficient at the boundary altitude, and the index of refraction of the air just above the boundary altitude. The pseudo extinction coefficient is defined to be the sum of the Rayleigh, aerosol, and Ozone coefficients. If the wavelength of the light being considered is in the range in which water vapor and CO_2 absorption is significant, provisions have been made for inputting amounts of the accumulated water vapor and accumulated CO_2 from ground level to the boundary altitude. If the water vapor and CO_2 concentrations are required, then the temperature and pressure for each boundary altitude are also required.

In addition to the division of the atmosphere into atmospheric layers, the FLASH program provides for the division of the atmosphere into as many as 10 aerosol scattering regions within each of which the aerosol size distribution remains constant even though the number density may vary. An aerosol scattering region is defined in the input by listing the altitudes of the upper and lower spherical surfaces bounding the region. A phase matrix number is also assigned to each aerosol scattering region indicating which of the normalized aerosol phase matrices in the problem input pertains to the aerosol size distribution within that region.

The source for the FLASH program is assumed to be an infinite plane parallel source tangent to the upper atmosphere at the zero polar position. The receiver positions are all at the same altitude but at different polar positions within the zero azimuthal plane.

3.3 Selection of Receiver View Angles

A set of solid angles of view are defined in the problem input data by listing the polar and azimuthal angles that bound each solid angle. The polar angles are measured from a radial through the receiver position with the zero polar angle along the outward radial, Fig. 2.

The total number of histories run with the FLASH program are divided equally among the polar angle intervals used to define the receiver solid angles of view. The number of histories run within a given polar angle interval is divided equally among the solid angles defined by the azimuthal angles bounds listed for that polar angle interval.

It is not necessary that view angles be defined to cover the 4π steradians about the receiver. Sampling may be confined to any desired solid angle or even to one or more discrete directions with the method used to define the solid angles of view.

The FLASH program is designed to sample backward photon histories from the solid angles of view systematically and to printout the scattered intensity for each solid angle of view before proceeding to the next.

At the start of each history before the history counter NHIST is incremented, the index of the polar angle interval, LA, and the azimuthal interval, LAZ, within the polar angle interval are determined with the following expressions:

$$\begin{aligned} LA &= 1 + NPVA * NHIST / NHMAX \\ JAZ &= NHIST - (LA - 1) * NHMAX / NPVA \\ LAZ &= 1 + NAZ(LA) * JAZ * NPVA / NHMAX \end{aligned}$$

where NHMAX is the total number of histories to be run, NPVA is the number of polar angle intervals used to define the solid angles of view, and NAZ(LA) is the number of solid angles of view in the LAth polar angle interval.

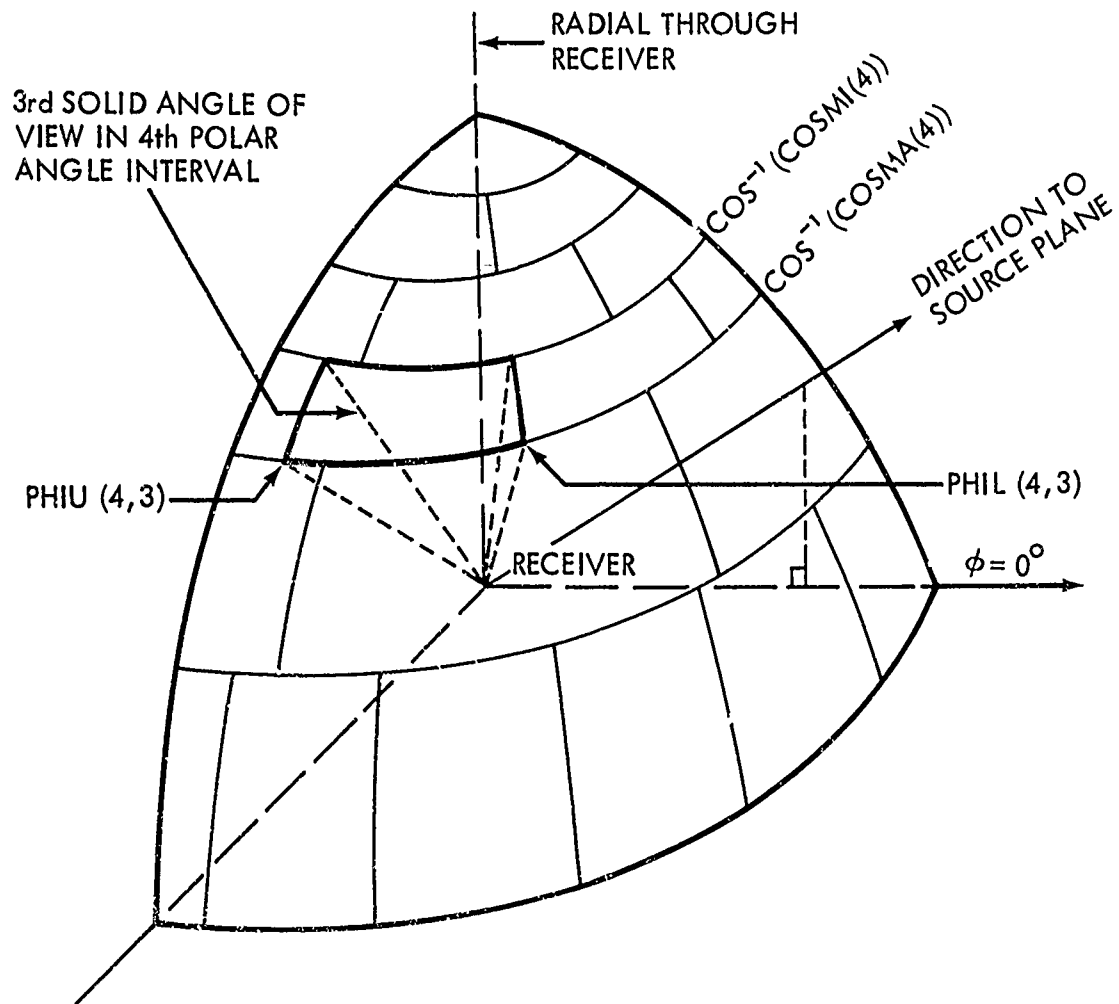


Fig. 2. Receiver View Angles

The discrete directions of the light entering the solid angle of view is sampled from a uniform distribution within the solid angle of view. The cosine, CGAM, of the polar angle of the light's direction entering the view angles is given by

$$CGAM = COSMI(LA) - RN * (COSMI(LA) - COSMA(LA))$$

where RN is a random number selected from a uniform distribution between 0.0 and 1.0, and COSMI(LA) and COSMA(LA) are the cosines of the lower and upper bounds of the polar angles bounding the LATH polar angle interval. The azimuthal direction, ALF, of the light entering the solid angle of view is given by

$$ALF = PHIL(LA, LAZ) + RN * (PHIU(LA, LAZ) - PHIL(LA, LAZ))$$

where RN is a random number, and PHIL(LA, LAZ) and PHIU(LA, LAZ) are the lower and upper azimuthal angle bounds of the LAZth solid angles of view in the LATH polar angle interval.

3.4 Distance to Collision

Once the initial direction of the photon's backward path is determined, the optical distance through each of the atmospheric layers that the particle traverses along a path to the upper or lower surface of the atmosphere is computed. The path followed by the particle is bent at each boundary between the atmospheric layers due to the change in the index of refraction from one layer to the next. If the particle's path intersects the ground surface before reaching the upper boundary of the atmosphere, the optical distance between collisions is chosen from the exponential distribution

$$SRHO = -\ln(1.0 - RN) ,$$

where SRHO is the sampled path length and RN is a random number chosen from a uniform distribution between 0.0 and 1.0. The random path length is then compared with the total optical distance computed for the particle's path from the receiver to the point where the path intersects the ground

surface. If the sampled pathlength is greater than the optical distance to the ground intersection, a reflection is forced to occur at the intersection point. If the random pathlength is less than the optical distance to the ground intersection, a collision is considered to occur at the point on the particle's path where the optical distance is equal to the sample pathlength.

If the particle's path intersects the upper boundary of the earth's atmosphere before intersecting the ground surface, the random pathlength between collisions is chosen from a truncated exponential distribution thus forcing a collision before the particle escapes the atmosphere. The random path is chosen with the expression

$$SRHO = -\ln(1.0 - RN * (1.0 - \exp(-ROMAX)))$$

where RN is a random number chosen from a uniform distribution between 0.0 and 1.0 and ROMAX is the optical distance along the particle's path from the receiver to the top of the atmosphere. When the collision is forced to occur before the particle escapes the atmosphere, the particle weight is adjusted to remove the bias introduced by forcing the collision with the expression

$$WATE = WATE(1 - \exp(-ROMAX)) ,$$

where WATE is the particle weight.

3.5 CO₂ and Water Vapor Absorption

If the wavelength of light being considered is one for which carbon dioxide or water vapor absorption is significant, the CO₂ transmissions are computed for a finite wavelength interval by first computing the equivalent CO₂ thickness between collisions for some standard temperature T₀ and pressure P₀ with the equation

$$c = \sum_i X_i \frac{P_i}{P_0} \frac{T_0}{T_i}$$

where X_i is the product of the CO_2 density times the distance traversed in the i th atmospheric layer, P_i is the pressure in the i th atmospheric layer, and T_i is the temperature in the i th atmospheric layer. Then, the CO_2 transmission is computed in FLASH with the expression (Ref. 13-14),

$$T(\lambda) = e^{-1.83(c*k(\lambda))^{0.73}}$$

The wavelength-dependent parameter $k(\lambda)$ is required as input to FLASH and must be determined from some known data for a given P_o and T_o , i.e. Ref. 15-16.

In the FLASH program, it is assumed that the effect of Rayleigh and aerosol scattering and ozone absorption for a small finite wavelength interval can be represented with monochromatic light for a wavelength within the interval, since the scattering and absorption coefficients for these processes vary fairly smoothly with wavelength. However, since CO_2 absorption varies quite radically with wavelength even within small intervals, up to 20 $k(\lambda)$ values may be input representing twenty smaller intervals within some larger interval and the average of the CO_2 transmission for the smaller intervals is computed to give the CO_2 transmissions for the larger interval.

FLASH uses a modification of the expression developed by Howard et. al. (Ref. 17), who fitted the Goody model to their water vapor absorption data to calculate the water vapor transmission.

$$T(\lambda) = \exp \sum_i \frac{-1.97 W_i/W_o(\lambda)}{\left(1 + 6.57 W_i/W_o(\lambda) \frac{P_o}{P_i} \left(\frac{T_i}{T_o}\right)^{1/2}\right)^{1/2}}$$

where $T(\lambda)$ is the transmission at wavelength λ , W_i is the product of the water vapor density times the distance traversed in the i th atmospheric layer, P_i is the pressure in the i th atmospheric layer and $W_o(\lambda)$ is the vapor length necessary to reduce the transmission to 50% at the pressure

P_0 and temperature T_0 . The water vapor transmission for some finite wavelength interval is then computed by averaging the transmission for as many as 20 subintervals as is the CO_2 transmission. The photon weight at each collision is multiplied by the average CO_2 and water vapor transmissions along the path between collisions to account for the water vapor and CO_2 absorption along that path.

3.6 Direction Before Collision

For each collision or reflection that occurs during the course of tracing the life history of the particle, the angle γ between the particle's direction before collision and a radial through the collision point is computed (Fig. 3). The angle α between the spherical projection of the particle's direction before collision and the spherical projection of the line joining the collision and receiver points is also calculated. In addition to the direction angles with respect to the radial through the collision or reflection point, the displacement from the receiver position is computed in terms of the two position angles θ and ϕ . Fig. 3 shows the displacement angles θ and ϕ , where θ is the angle between the radial through the receiver and the radial through the collision or reflection point and ϕ is the angle at the receiver between the zero azimuth and a spherical projection of a line joining the receiver and the collision point. The cosine of the displacement angle, CTHEN, is given by the expression

$$\text{CTHEN} = \text{CTHE} * \text{CDTHE} - \text{STHE} * \text{SDTHE} * \text{CALF} ,$$

where CTHE and STHE are the cosine and sine of the displacement angle at the previous collision or reflection, CDTHE and SDTHE are the cosine and sine of the angle at the earth's center subtending the pathlength between the current and previous collisions, and CALF is the cosine of the angle between the spherical projection of the pathlength between collision and the spherical projection of the line joining the previous collision and the receiver position. The cosine, CALFN, of the angle

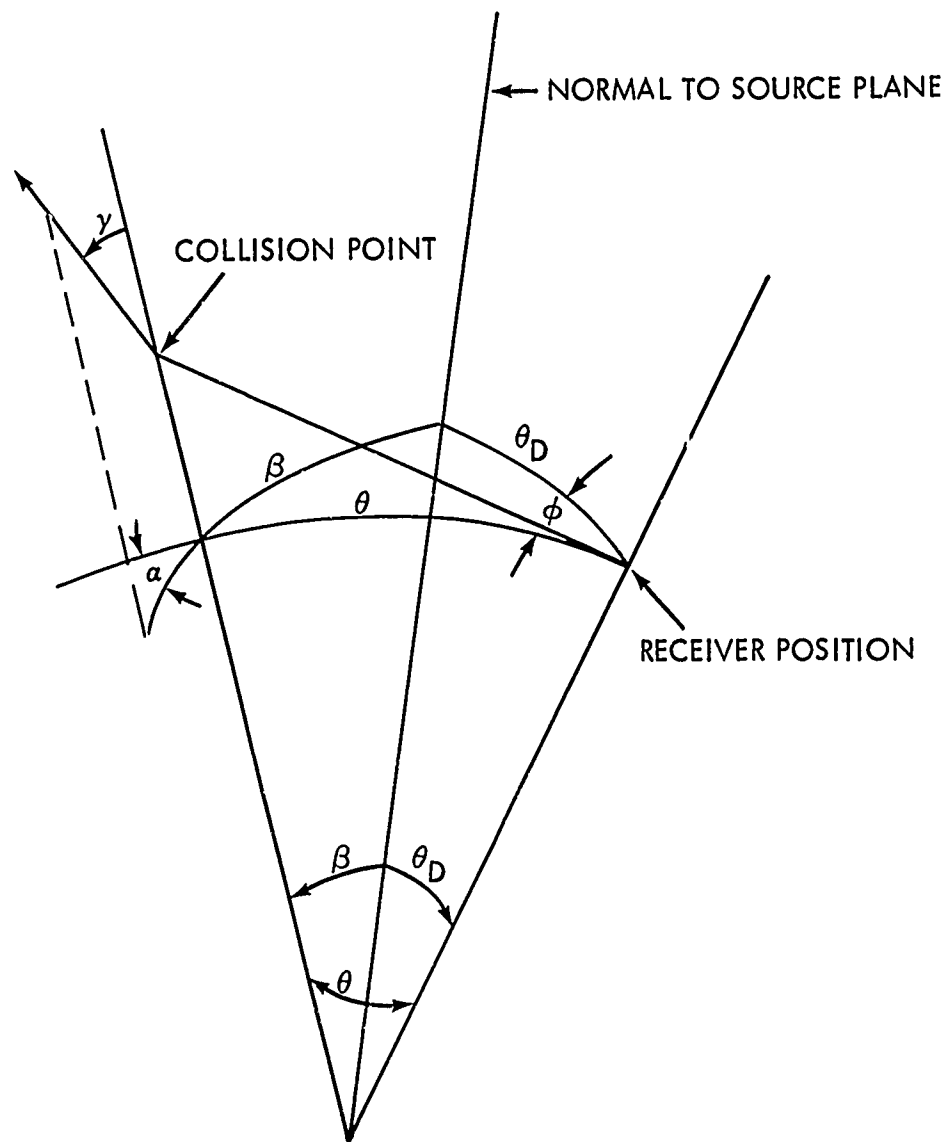


Fig. 3. Displacement Angles

between the spherical projection of the pathlength and the spherical projection of the line joining the current collision with the receiver position is given by the expression

$$CALFN - (CTHE - CDTHE * CTHE) / (SDTHE * STHE) ,$$

where the sine and cosine values are defined as above.

3.7 Effects of Changes in Index of Refraction

The direction that a photon travels between collisions is modified as it passes from one atmospheric layer to the next by the change in the index of refraction. If λ is the angle between the photon's direction and the radial through the point of intersection with an atmospheric layer boundary, the angle is modified by the expression $\lambda' = \sin^{-1}((n/n')\sin\lambda)$, where λ' is the angle the photon direction makes with the radial through the intersection point after crossing the boundary and n and n' are the indices of refraction for the original and new atmospheric layers. In the case that $\sin\lambda$ is approximately 1.0 and $n/n' > 1$ so that $\sin\lambda'$ becomes greater than 1.0, $\sin\lambda'$ is set equal to 1.0 and the photon leaves the spherical surface in a tangential plane.

3.8 Selection of the Scattering Event

Each time a collision or reflection position is determined, the FLASH program locates the atmospheric layer containing the collision center and interpolates between the scattering-to-pseudo extinction coefficient ratios and the Rayleigh-to-scattering coefficient ratios for the bounds of the layer to find the scattering-to-pseudo extinction coefficient ratio and the Rayleigh-to-scattering coefficient ratio for the collision altitude. The photon weight is multiplied by the scattering-to-pseudo extinction coefficient ratio to account for the fact that no ozone or aerosol absorption of the photon is allowed. The type of scattering event is determined to be either a Rayleigh or an aerosol scattering event by comparing a random number with the ratio of the Rayleigh-to-scattering

coefficient. If the random number is less than the ratio, the scattering event is assumed to be a Rayleigh event, otherwise it is assumed to be an aerosol scattering event.

3.9 Selection of Direction to Source

Once the position of a collision or a reflection relative to a receiver position has been determined and the direction angles of the photon before collision have been calculated, then the direction that the photon must take in order to intersect the source plane at an angle of 90 degrees is determined. Due to the bending of the photon's path by the change in the atmospheric index of refraction with altitude, an iterative process was developed to determine the initial direction to start the photon path so that it will intersect the source plane at a right angle. The iterative process is described below.

The position of the collision relative to the zero polar axis is computed with the expression:

$$\cos\beta = \cos\theta\cos\theta_D + \sin\theta\sin\theta_D\cos\phi ,$$

where β is the angle between the radial through the collision position and the zero polar axis, θ and ϕ are the polar and azimuthal displacement angles from the receiver located at polar position θ_D . If it were not for the bending of the photon path, a light ray emitted normal to the source plane so that it passes through the collision center would intersect the radial through the collision center at the angle β , Figure 4. The iterative process used to determine the angle of intersection between the radial and the curved path from the source plane to collision first starts the photon path from the collision position toward the source plane in the direction β , Figure 4. The angle of intersection of the curved path with the source plane is then determined. The difference between the angle of intersection and 90 degrees, ϵ , is computed and this difference is tested to determine whether the angle of intersection is sufficiently close to 90 degrees to be considered an intersection at right angles. If ϵ is too

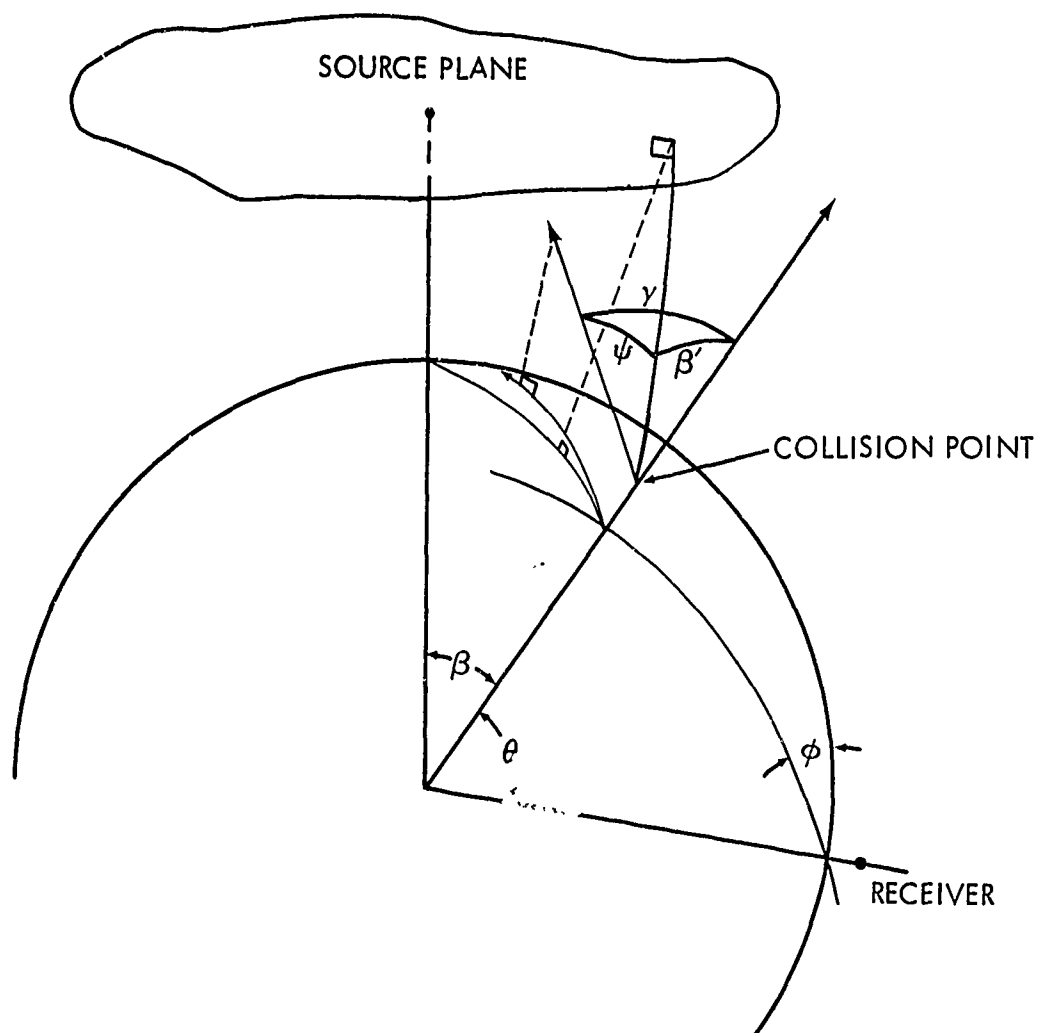


Fig. 4. Geometry for Calculation of Scattering Angle between Direction to Source Plane and Direction before Collision

large it is subtracted from the angle β and a photon path from the collision point is started in the direction of $\beta' = \beta - \epsilon$. The angle of intersection of the second photon path and the source plane is computed and tested as discussed above. This process is repeated until the angle between the intersection of the photon's path and the source plane is within an acceptable interval about 90 degrees.

3.10 Polarization Parameters After Scattering

Next the scattering angle between the direction of propagation before collision and the direction of the curved path normal to the source plane is computed, Figure 4. The cosine of the scattering angle, CSA, is given by the expression

$$CSA = CBETP * CGAM + SBETP * SGAM * CPHIP ,$$

where CBETP and SBETP are the cosine and sine of the angle between the radial through the collision point and the direction of the curved path normal to the source plane, CGAM and SGAM are the cosine and sine of the angle between the photon's direction before collision and a radial through the collision point, and CPHIP is the cosine of the angle between the spherical projection of the photon's directions before and after collision.

In order to determine the magnitude of the four polarization parameters in a plane containing the polar axis and the direction of the photon through the source plane the polarization parameters are rotated into the plane of scatter from the plane containing the direction before collision and the radial through the collision point. The sine and cosine of the rotation angle for the polarization parameters is computed with the equations

$$\begin{aligned} SROT &= SBETP * SPHIP / SSA \\ CROT &= (CBETP - CSA * CGAM) / (SSA * SBETP) , \end{aligned}$$

where SSA is the sine of the scattering angle and SPHIP is the sine of

the angle between the spherical projections of the photon's directions before and after collision.

The polarization parameters I_{\parallel} , I_{\perp} , U and V before rotation are transformed to

$$I_{\parallel}' = I_{\parallel} * \text{CROT}^2 + I_{\perp} * \text{SROT}^2 + 0.5 * U * \text{S2ROT}$$

$$I_{\perp}' = I_{\parallel} * \text{SROT}^2 + I_{\perp} * \text{CROT}^2 - 0.5 * U * \text{S2ROT}$$

$$U' = I_{\perp} * \text{S2ROT} - I_{\parallel} * \text{S2ROT} + U * \text{C2ROT}$$

$$V' = V$$

after rotation through the angle whose sine and cosine are SROT and CROT. S2ROT and C2ROT are the sine and cosine of an angle twice the magnitude of the rotation angle.

If the Rayleigh process is chosen for the scattering event, the polarization parameters after scattering through the angle whose cosine is CSA are

$$I_{\parallel r}' = (3/16\pi) * \text{CSA}^2 * I_{\parallel}'$$

$$I_{\perp r}' = (3/16\pi) * I_{\perp}'$$

$$U_r' = (3/16\pi) * \text{CSA} * U'$$

$$V_r' = (3/16\pi) * \text{CSA} * V' ,$$

where $I_{\parallel r}'$, $I_{\perp r}'$, and U_r' and V_r' are the polarization parameters after Rayleigh scattering. If the scattering event was an aerosol event, the polarization parameters after scattering are defined by

$$I_{\parallel a}' = i_2(\theta) * I_{\parallel}'$$

$$I_{\perp a}' = i_1(\theta) * I_{\perp}'$$

$$U_a' = i_3(\theta) * U' - i_4(\theta) * V'$$

$$V_a' = i_4(\theta) * U' + i_3(\theta) * V' ,$$

where $I'_{||a}$, $I'_{\perp a}$, U'_a and V'_a are the polarization parameters after aerosol scattering and $i_1(\theta)$, $i_2(\theta)$, $i_3(\theta)$, and $i_4(\theta)$ are the four elements of the aerosol phase matrix evaluated at the scattering angle $\theta = \cos^{-1}(\text{CSA})$.

3.11 Estimate of the Scattered Intensity

An estimate of the scattered light intensity at a receiver is obtained by multiplying the photon weight after the collision by the sum of the first two polarization parameters times the attenuation along the path from the source plane to the collision.

$$\text{EST} = \text{WATE} * (I'_{||} + I'_{\perp}) * \exp(-\text{ROMAX}) ,$$

where WATE is the photon weight after collision, $I'_{||}$ and I'_{\perp} are the parallel and perpendicular components of the polarization parameters scattered into the direction of the curved path that intersects the source plane at right angles, and ROMAX is the optical distance along the path from the collision to the source plane.

3.12 Selection of Direction to Previous Collision

After the estimate of the scattered light intensity at the receiver from a given collision is made, the FLASH program selects an angle of scatter in order to trace the photon through the next order of scattering. The scattering angle depends upon whether the scattering event was determined to be a Rayleigh or an aerosol event.

For either process, the orientation of the scattering plane is selected from a uniform distribution between 0 and 2π . The polarization parameters are rotated into the scattering plane using the expressions:

$$\begin{aligned} I'_{||} &= I_{||} \cos^2 \phi + I_{\perp} \sin^2 \phi + 0.5U \sin 2\phi \\ I'_{\perp} &= I_{||} \sin^2 \phi + I_{\perp} \cos^2 \phi - 0.5U \sin 2\phi \\ U' &= I_{\perp} \sin 2\phi - I_{||} \sin 2\phi + U \cos 2\phi \\ V' &= V \end{aligned}$$

where $I'_{||}$, I'_{\perp} , U' , and V' are the polarization parameters in the scattering plane, $I_{||}$, I_{\perp} , U , and V are the polarization parameters in the reference plane before rotation and ϕ is the angle between the reference plane and the scattering plane.

If the Rayleigh process is chosen for the scattering event, the scattering angle is chosen from the density function

$$P(\theta) = 3/8(1+\cos^2\theta)\sin\theta d\theta,$$

and the Rayleigh phase matrix is applied with the following equations

$$I'_{||r} = 2\cos^2\theta I'_{||} / (I'_{||} + I'_{\perp})$$

$$I'_{\perp r} = 2I'_{\perp} / (I'_{||} + I'_{\perp})$$

$$U'_r = 2U' \cos\theta / (I'_{||} + I'_{\perp})$$

$$V'_r = 2V' \cos\theta / (I'_{||} + I'_{\perp}),$$

where $I'_{||r}$, $I'_{\perp r}$, U'_r , and V'_r are the polarization parameters after scattering through the angle θ and $I'_{||}$, I'_{\perp} , U' , and V' are the polarization parameters in the scattering plane before scattering.

If the Mie process is chosen for the scattering event, the scattering angle is chosen from the density function

$$\frac{R_{\perp} i_1(\theta) + R_{||} i_2(\theta)}{\sigma_s} \sin\theta d\theta,$$

where $R_{\perp} = \frac{I'_{\perp}}{I'_{\perp} + I'_{||}}$, $R_{||} = \frac{I'_{||}}{I'_{\perp} + I'_{||}}$ and $i_1(\theta)$ and $i_2(\theta)$ are the elements of the aerosol phase matrix relating to the perpendicular and parallel components of the intensity as computed with Mie theory. The aerosol phase matrix is then applied to the polarization parameters through the following equations to yield the value of the polarization parameters after scattering:

$$\begin{aligned}
 r'_{\parallel a} &= 2I'_{\parallel} i_2(\theta) / (i_1(\theta) + i_2(\theta)) \\
 I'_{\perp a} &= 2I'_{\perp} j_1(\theta) / (i_1(\theta) + i_2(\theta)) \\
 U'_a &= 2(U' i_3(\theta) - V' i_4(\theta)) / (i_1(\theta) + i_2(\theta)) \\
 V'_a &= 2(U' i_4(\theta) + V' i_3(\theta)) / (i_1(\theta) + i_2(\theta)) .
 \end{aligned}$$

The parameters $I'_{\parallel a}$, $I'_{\perp a}$, U'_a , and V'_a are defined in the plane of scatter. The angle ϕ' between the scattering plane and the new reference plane containing the direction of propagation after scatter and the vertical vector is calculated with the trigonometric relationships for spherical triangles. The four parameters are then rotated through this angle using the expressions for rotating the parameters given previously.

3.13 Ground and Cloud Reflection

If the photon is reflected from the ground or a cloud surface, the FLASH program selects the direction after reflection from a reflection distribution rather than from the Rayleigh or aerosol phase matrix.

Once it has been determined that the photon intersected a reflection surface, the indices of refraction for the two materials on either side of the reflection boundary are checked to determine whether specular reflection is possible. If both indices are the same, specular reflection is not possible; but if they are different, the reflection coefficients for the parallel and perpendicular components of the specular reflectance are computed with the expressions:

$$\begin{aligned}
 r_{\parallel} &= (N_I \cos \gamma_R + N_R \cos \gamma_I) / (N_I \cos \gamma_R - N_R \cos \gamma_I) \\
 r_{\perp} &= (-N_I \cos \gamma_I + N_R \cos \gamma_R) / (-N_I \cos \gamma_I + N_R \cos \gamma_R) ,
 \end{aligned}$$

where N_I and N_R are the indices of refraction for the materials containing the incident and refracted rays respectively and γ_I and γ_R are the angle of incidence and the angle of refraction, respectively. The probability of specular reflectance is given by

$$PR = I_{\parallel} r_{\parallel}^2 + I_{\perp} r_{\perp}^2 .$$

A random number is generated and if the random number is less than PR, the reflection is assumed to be specular. If the random number is greater than PR, reflection is assumed to be diffuse.

If the reflection is determined to be specular, the polarization parameters are modified by the expressions:

$$I_{\parallel}' = r_{\parallel}^2 I_{\parallel} / PR$$

$$I_{\perp}' = r_{\perp}^2 I_{\perp} / PR$$

$$U' = r_{\perp} r_{\parallel} U / PR$$

$$V' = r_{\perp} r_{\parallel} V / PR$$

If the reflection event is determined not to be specular, then the reflection angle can be sampled from an isotropic or cosine distribution or from an arbitrary distribution defined by a set of tabulated input data. Non specular reflected light is assumed to be unpolarized so the polarization parameters for the reflected photon are given by

$$I_{\parallel}' = \alpha (I_{\perp} + I_{\parallel}) / 2.0$$

$$I_{\perp}' = \alpha (I_{\perp} + I_{\parallel}) / 2.0$$

$$U' = 0.0$$

$$V' = 0.0 \quad ,$$

where I_{\parallel} and I_{\perp} are the parallel and perpendicular components of the intensity associated with the incident photon, and α is the diffuse albedo for the reflection surface.

IV. FLASH CALCULATIONS

In order to validate the backward Monte Carlo approach used in the FLASH program, comparisons of FLASH results with several other calculations have been made.

4.1 Comparison for Rayleigh Scattering

The first of these was a comparison of the transmitted intensities through a unit optical thickness pure Rayleigh atmosphere with the results reported by Coulson et. al. in Ref. 9. For the FLASH calculations receivers were positioned at ground level and at polar positions such that the uncollided light from the plane parallel source would intersect the radials through the receivers at zenith angles whose cosines were 0.92, 0.8, 0.6, 0.4, 0.2, and 0.1. The FLASH calculated average scattered intensity multiplied by 2π is compared in Table I with 2π times the average scattered intensity obtained by integrating Coulson et. al.'s transmitted intensity data over receiver solid angle for the same set of incident zenith angles. As one would expect, the data for the two atmospheres are in reasonably good agreement until the incident angle becomes large and then the data for the spherical shell geometry tends to over-predict that for the plane geometry. The polar angular distributions of the scattered intensities for the 0.0 and 0.8 ground albedos are compared for the incident angles of $\cos^{-1}0.92$ and $\cos^{-1}0.4$ in Figures 5 and 6. Although the statistical fluctuations of the Monte Carlo data are largely due to the small sample size of 1120 histories, the Monte Carlo data does follow the same general trend as does Coulson's data.

Table I

COMPARISON OF SCATTERED LIGHT INTENSITY TRANSMITTED THROUGH SPHERICAL
AND PLANE RAYLEIGH ATMOSPHERES OF A UNIT OPTICAL THICKNESS

Cosine Incident Angle	Albedo	<u>2π * AVERAGE SCATTERED INTENSITY</u>	
		Spherical	Plane
0.92	0.0	0.606	0.588
	0.8	1.411	1.373
0.80	0.0	0.660	0.641
	0.8	1.424	1.385
0.60	0.0	0.745	0.711
	0.8	1.426	1.373
0.40	0.0	0.798	0.736
	0.8	1.377	1.291
0.20	0.0	0.757	0.640
	0.8	1.213	1.068
0.10	0.0	0.665	0.535
	0.8	1.092	0.897

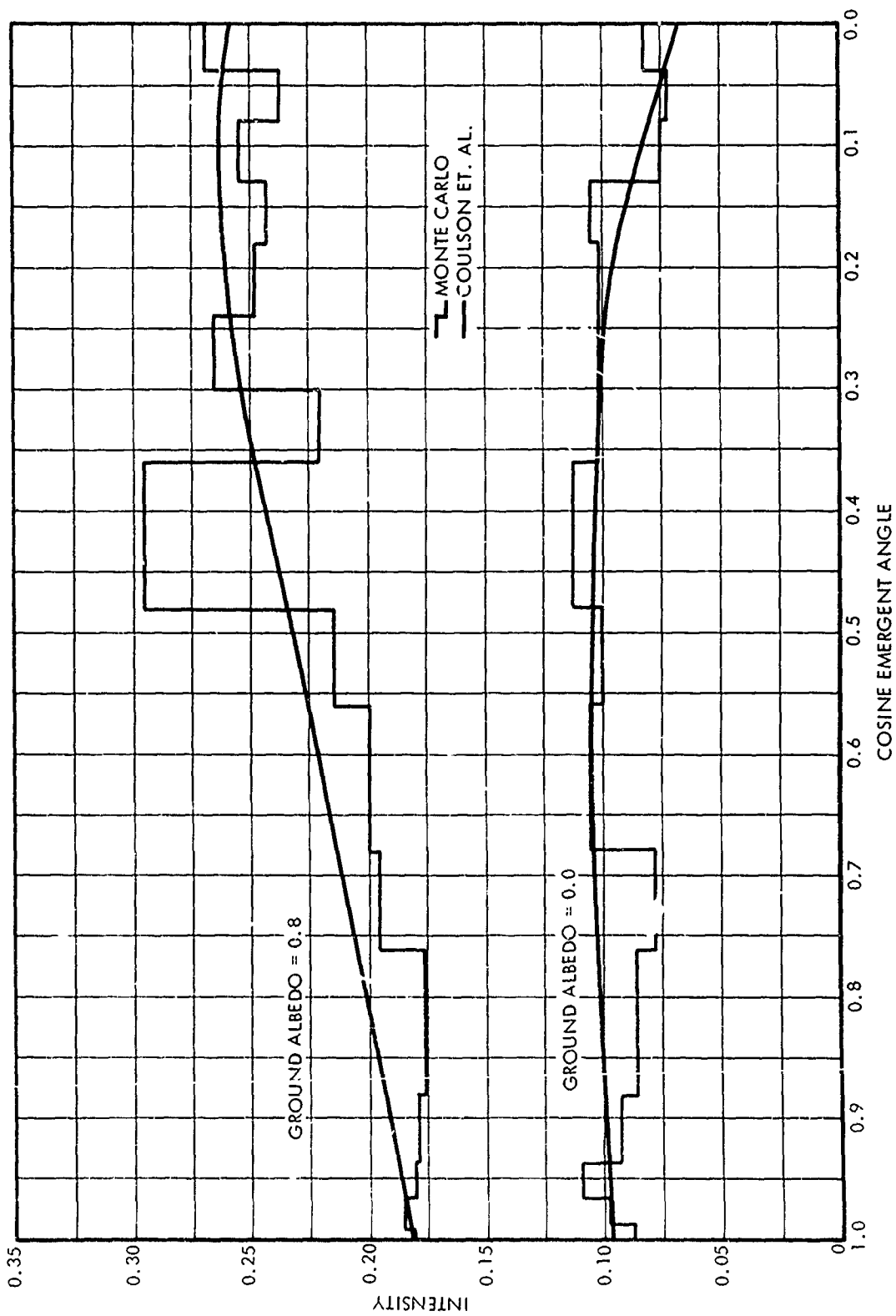


Fig. 5. Intensity Transmitted through a Rayleigh Atmosphere of Unit Optical Thickness: Plane Parallel Source Incident at Arc Cosine = 0.92

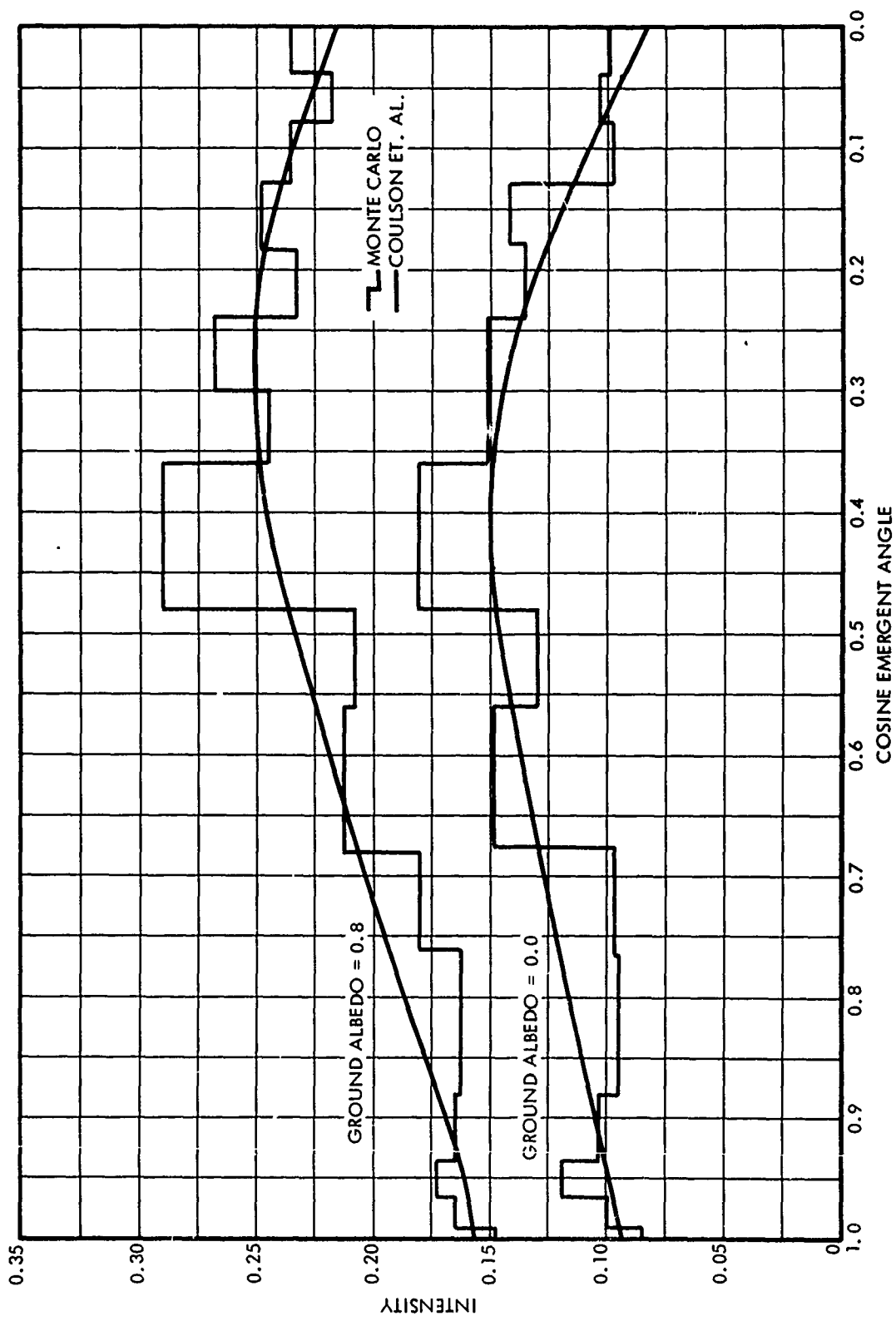


Fig. 6. Intensity Transmitted through a Rayleigh Atmosphere of Unit Optical Thickness: Plane Parallel Source Incident at Arc Cosine = 0.4

4.2 Comparison for Aerosol Scattering

The second test problem to check the validity of the FLASH program was for an atmosphere containing aerosols (Ref. 5). The Rayleigh attenuation coefficients for the hazy atmosphere were assumed to be those given by Elterman for a clear standard atmosphere (Ref. 18). Also the ozone absorption coefficients for 0.55 μ light reported in Ref. 5 for the clear standard atmosphere were used to define the ozone absorption as a function of altitude in the atmosphere described below.

The aerosol attenuation coefficient profile used for the hazy atmosphere is shown in Figure 7 for the 0.55 μ wavelength light. The atmosphere was defined with a discontinuity at 3 km altitude in the aerosol attenuation coefficient profile. Below 3 km altitude, the aerosol attenuation coefficient profile was assumed to vary exponentially with altitude according to the profile reported in Ref. 5 after being normalized to give a meteorological range of 3 km at ground level. Above 3 km altitude, the aerosol attenuation coefficient was assumed to vary with altitude in the manner described by the average of 105 profiles determined by Elterman from searchlight measurements taken in New Mexico during 1963 and 1964 (Ref. 19). The profile obtained from the average of 105 profiles was normalized so that its magnitude when extrapolated by use of the profile in Ref. 5 to ground level would give a ground level meteorological range of 25 km. The profiles for 0.55 μ wavelength light above and below 3 km altitude were normalized to ground level meteorological ranges with use of the expression

$$\sigma_a = (3.9/V) - \sigma_R$$

where σ_a is the aerosol attenuation coefficient, V is the meteorological range in kilometers, and σ_R is the Rayleigh attenuation coefficient at ground level for 0.55 μ wavelength light.

The aerosol size distribution below the haze layer was taken to be proportional to $r^{-2.5}$ while the distribution above the haze layer was

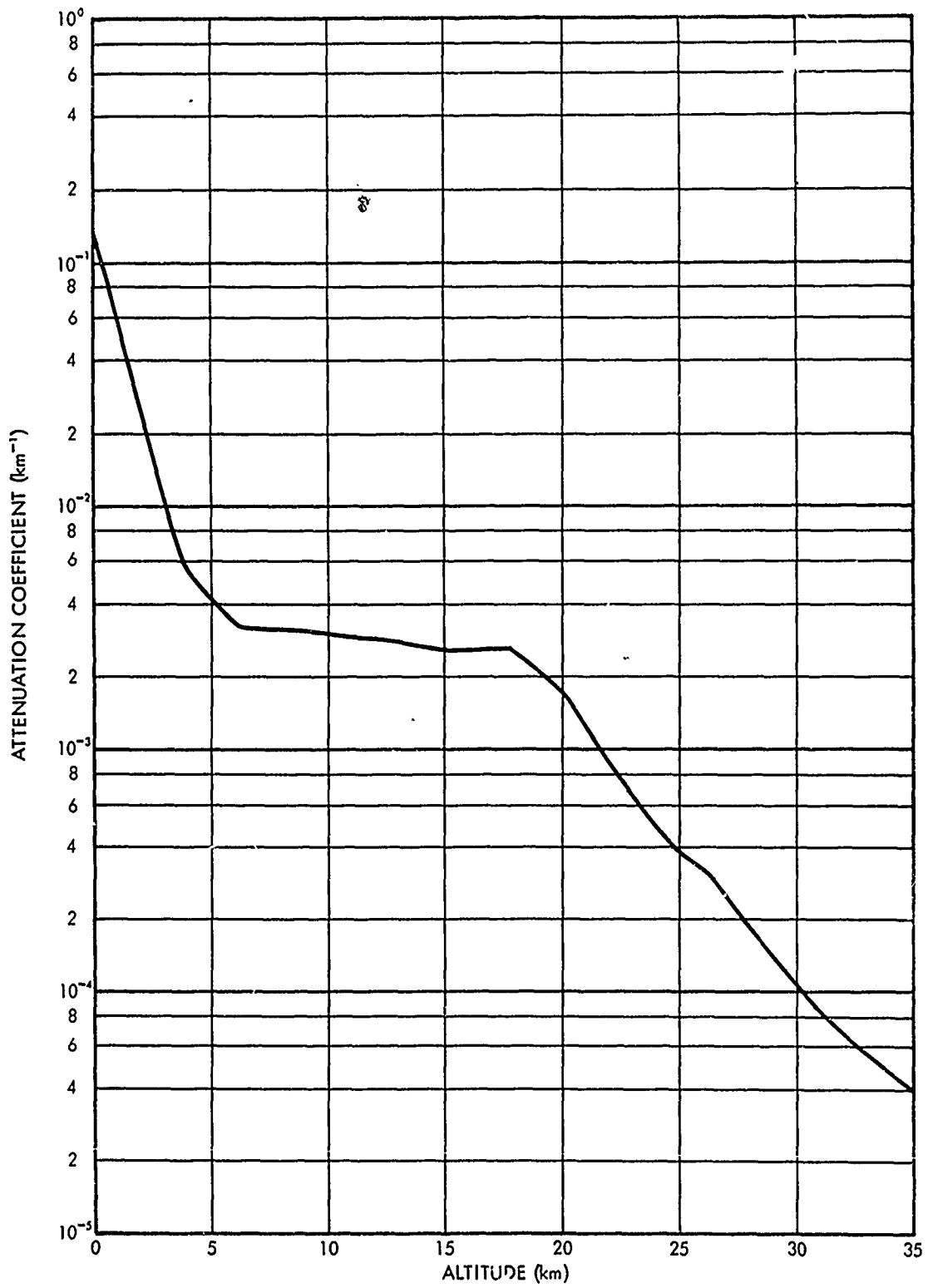


Fig. 7. Distribution with Altitude of the Aerosol Attenuation Coefficient for 0.55μ Wavelength Light in the Model Clear Atmosphere

taken to be proportional to $r^{-3.5}$ where r is the radius of the aerosol particle. Aerosol phase matrices were computed for the aerosol size distributions proportional to $r^{-2.5}$ and $r^{-3.5}$ by integrating the phase matrices calculated for spherical particles with a real index of refraction of 1.33 over the size range from 0.03 to 10μ .

A Lambert type ground surface was assumed and scattered intensities were calculated for ground albedo values of 0.0 and 0.8.

The scattered light intensities computed for the 10 kilometer altitude in the spherical atmosphere discussed above are compared in Table II with the scattered intensities computed for the 10 kilometer altitude in a similar planetary atmosphere with the LITE-IV Monte Carlo program. The agreement between the two sets of data is within 20 percent for nearly all incident angles except for the light incident at 87.5 degrees. This is thought to be a reasonable comparison considering the fact that the data shown for the FLASH program were obtained with a sample size of only 960 histories.

4.3 Intensity Emerging from Earth's Atmosphere

As a further check out of the calculational methods used in FLASH, two problems were run to calculate the scattered light intensity at a satellite orbiting at 300 nautical miles above the earth. The atmosphere, which was modeled by a clear maritime atmosphere, has a ground level visibility of 25 kilometers. The variation of the aerosol number density with altitude was taken to be that given by the Elterman 1968 model. The aerosol size distribution was assumed to be Deirmendjian's Haze M model. Calculations were made for satellite positions defined in terms of the earth angle which is the angle between the radials through the satellite position and the sun's position. The intensities for 0.37 micron and 0.78 micron wavelength light when the ground albedo was taken to be 0.0 and 0.8 are compared with the results from the RRA-89 program (Ref. 21) in Figures 8 and 9.

Table II

COMPARISONS OF SCATTERED LIGHT AT 10 KILOMETER ALTITUDE IN A HAZY
ATMOSPHERE FROM PLANE AND SPHERICAL GEOMETRY CALCULATIONS

Incident Angle (Degrees)	Albedo	<u>2π * AVERAGE SCATTERED INTENSITY</u>	
		Spherical	Plane
0	0.0	0.411	0.345
	0.8	1.498	1.533
15	0.0	0.419	0.350
	0.8	1.459	1.575
30	0.0	0.504	0.432
	0.8	1.500	1.606
45	0.0	0.806	0.605
	0.8	1.769	1.684
60	0.0	1.009	1.008
	0.8	1.848	1.922
75	0.0	1.848	1.808
	0.8	2.333	2.443
87.5	0.0	2.698	1.900
	0.8	2.990	2.184

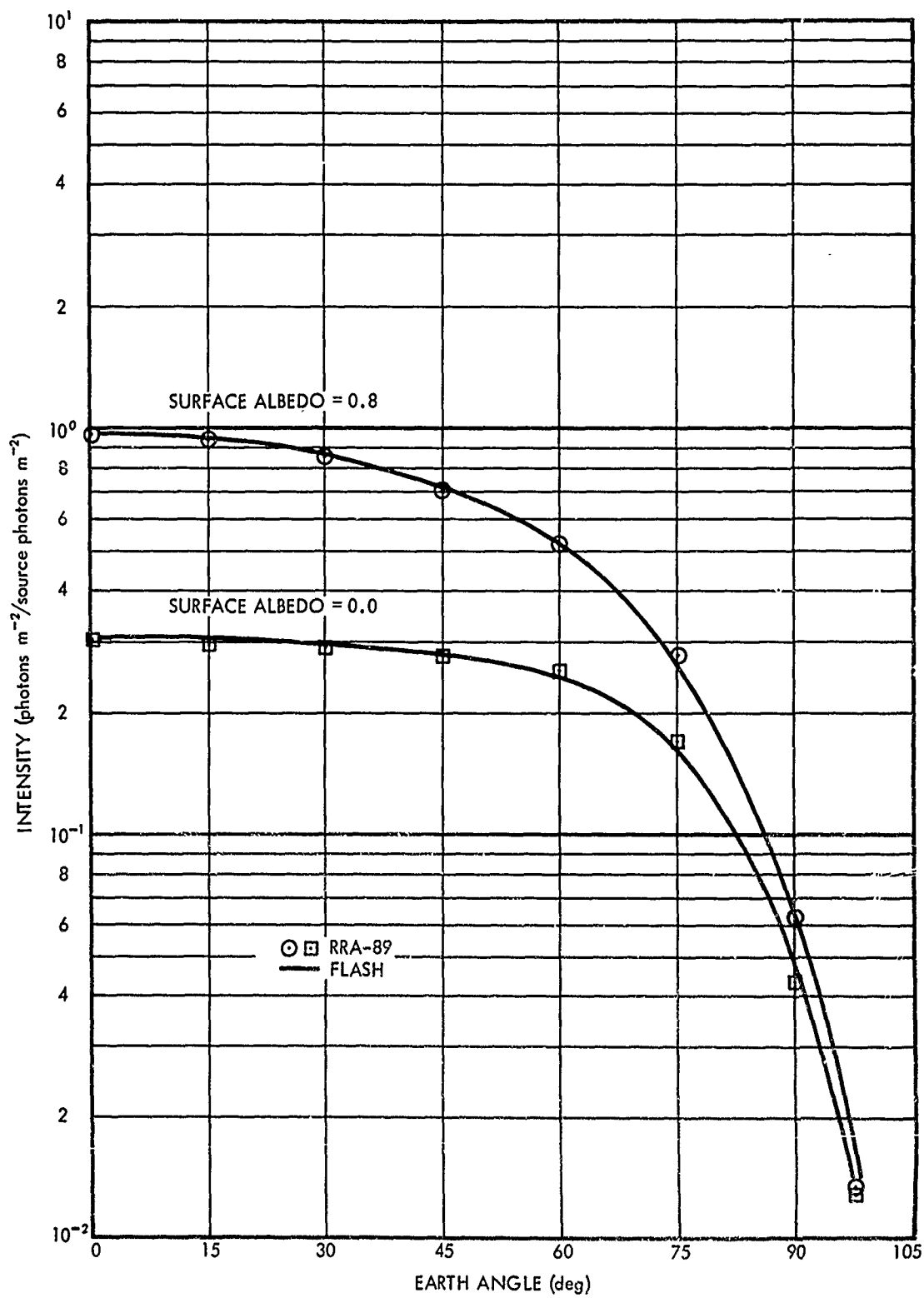


Fig. 8. Comparison of Data from a RRA-89 Calculation with Data from a Flash Calculation for a Wavelength of 0.37μ

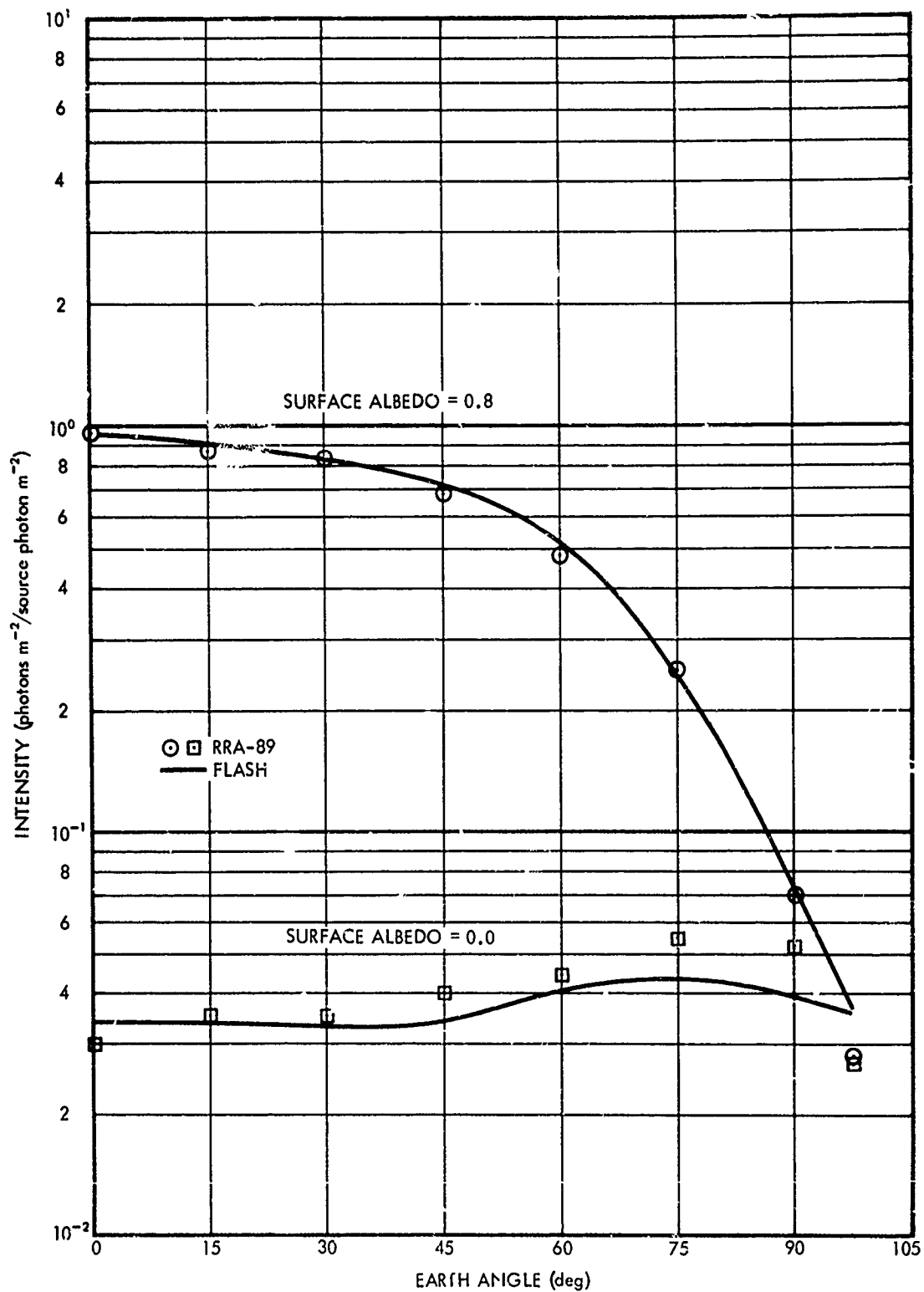


Fig. 9. Comparison of Data from a RRA-89 Calculation with Data from a Flash Calculation for a Wavelength of 0.78μ

The RRA-89 procedure was originally developed for the purpose of providing a method of computing the monochromatic light intensities above model atmospheres that result from atmospheric scattering and diffuse reflection by the ground surface. The calculational method used in RRA-89 is based on the use of atmospheric reflection data generated by use of the LITE-II procedure for plane parallel atmospheres in a machine procedure that determines the polar and azimuthal angle distributions of the light intensities at a satellite located above the atmosphere for arbitrary satellite position and direction to the sun. The comparisons shown in Figures 8 and 9 indicate that results obtained from the FLASH procedure are in good agreement with data from RRA-89 calculations.

4.4 Twilight Studies

The FLASH program was utilized in a study of twilight radiation for wavelengths of 0.5 and 0.7 microns for three atmospheric models. The three model atmospheres all contain the Rayleigh and ozone profiles given by Elterman in Reference 18. The aerosol profiles for the model atmospheres are shown in Fig. 10 for 0.55 micron wavelength light. Profile A is the Elterman 1964 aerosol profile for a clear atmosphere. Profile B is a modification of the Elterman 1968 profile for normal volcanic dust, and profile C is a strong enhancement of the volcanic dust in the 10 to 20 kilometers altitude range of the Elterman 1968 profile. The three profiles were normalized to the ground level aerosol coefficient for 0.5 μ and 0.7 μ given by Elterman in Ref. 18. The scattered light intensity was calculated for collimated receivers at ten meters altitude and pointing 20 degrees elevation in the plane of the sun. The receivers were placed at sun depression angles of 0, 2, 4, 5, 6, and 7 degrees. Figures 11 and 12 show the single and multiple scattered intensity as a function of sun depression angle for the 0.7 micron wavelength light in Atmospheres A and C. The difference between the single and multiple scattering is seen to be greater for the clear atmosphere, Fig. 11, than in the atmosphere with the high concentrations of volcanic dust, Fig. 12.

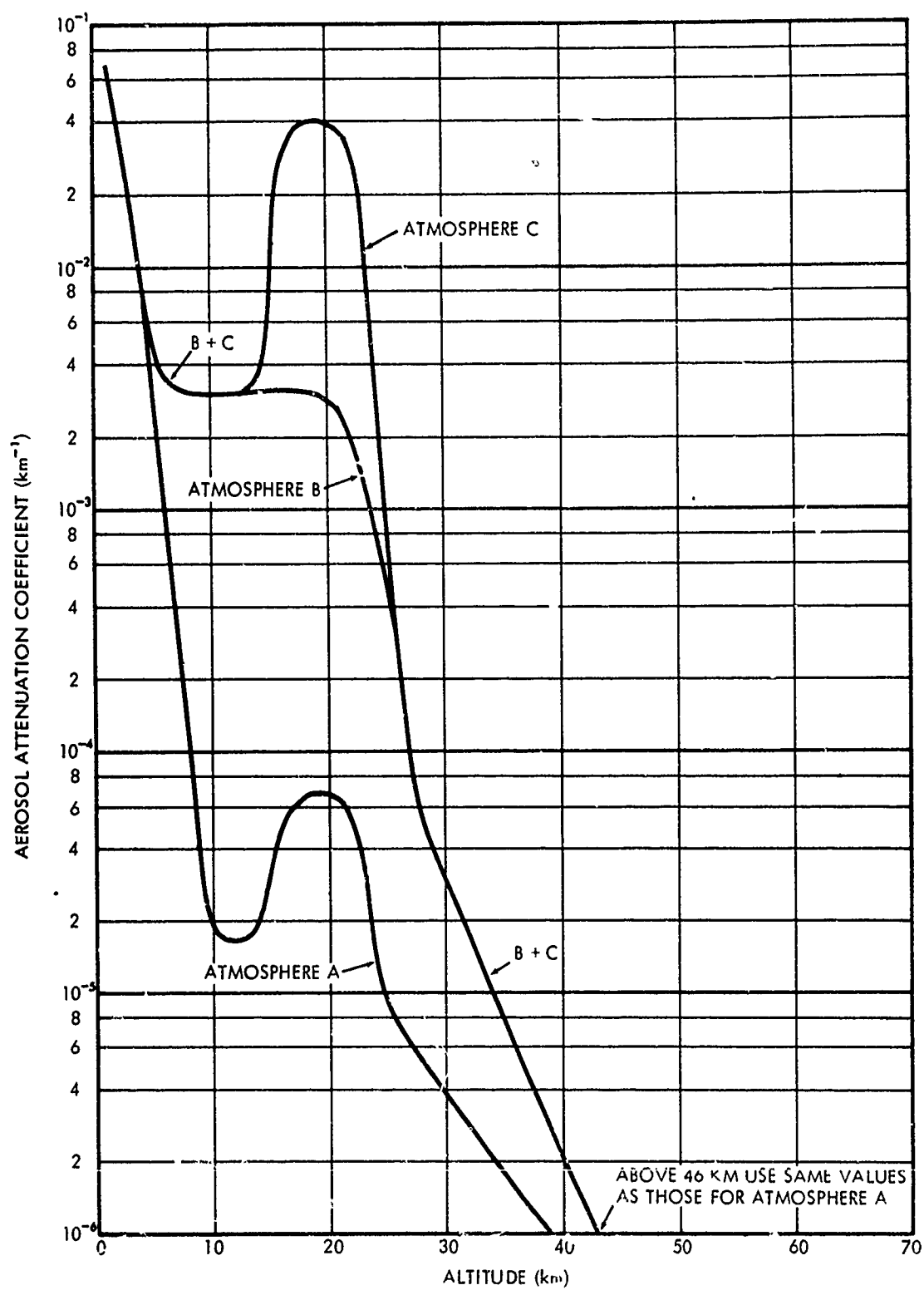


Fig. 10. Aerosol Attenuation Profiles used in Twilight Studies

It is seen in Figs. 11 and 12 that the single scattered intensities at the receivers for Atmospheres A and C do not differ significantly for a given sun depression angle. The importance of increased aerosol scattering that takes place in the dust layer between 5 and 25 km altitude in Atmosphere C is off set by the increased attenuation on the photon's path through the atmosphere. To better see what is happening to the light as it undergoes single collision events in the atmosphere, the FLASH procedure was modified so as to print out the intensity scattered per km of altitude as a function of altitude. Fig. 13 shows the results obtained for 0.7μ wavelength light undergoing single scattering in Atmospheres A and C. It is seen that the lower attenuation in Atmosphere A results in a larger single scattered intensity over that observed for Atmosphere C in the first 20 km of altitude. The importance of the dust layer between 15 and 25 km altitude in Atmosphere C is noted by the large single scattered intensity coming from those altitudes. Above 30 km altitude the increased attenuation of the single scattered radiation is noted for Atmosphere C over that computed for Atmosphere A as the single scattered light passes through lower altitudes on its way to the receiver. Thus, it is observed that although increased aerosol single scattering takes place within the dust layer centered around 20 km altitude in Atmosphere C, the increased attenuation resulting from that dust layer significantly reduces the magnitude of the single scattered intensity reaching the receiver.

An analysis of the FLASH multiple scattering calculations indicated that most of the multiple scattered intensity at the receiver position comes from photons that undergo multiple scattering in the first 10 km altitude in both Atmospheres A and C. The fact that the number of photons undergoing single scattering events in the first 10 km altitude is greater for Atmosphere A than for Atmosphere C (Fig. 13) explains why multiple scattering is more important for Atmosphere A than it is for Atmosphere C.

Additional studies on the effect of dust layers and multiple scattering on the light observed at a receiver as a function of sun depression angle, receiver view angle, and wavelength are being continued under contract F19628-70-C-0156.

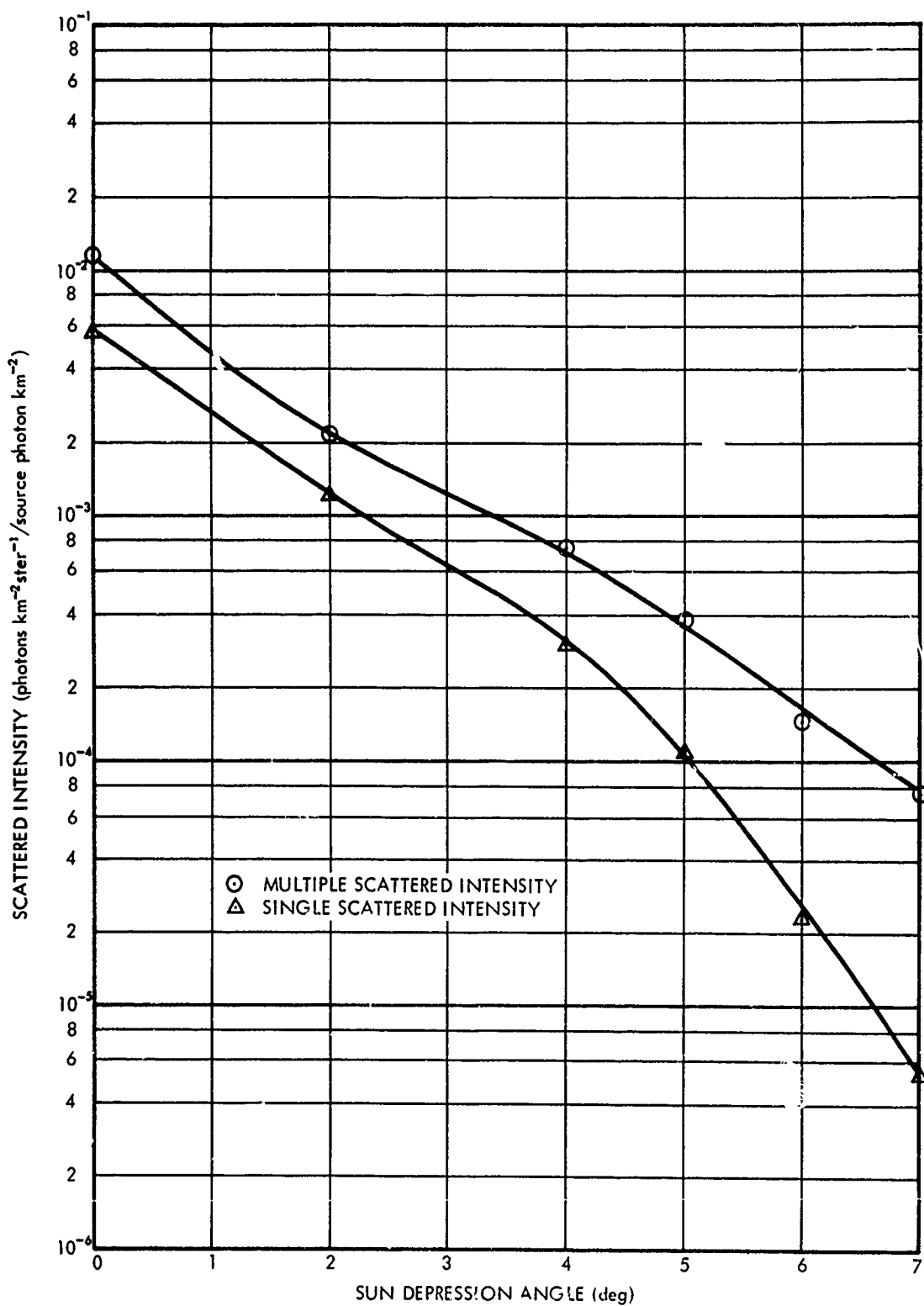


Fig. 11. Scattered Light Intensity at 20 Degrees Elevation versus Sun Depression Angle for Aerosol Profile A: 0.7μ Wavelength Light

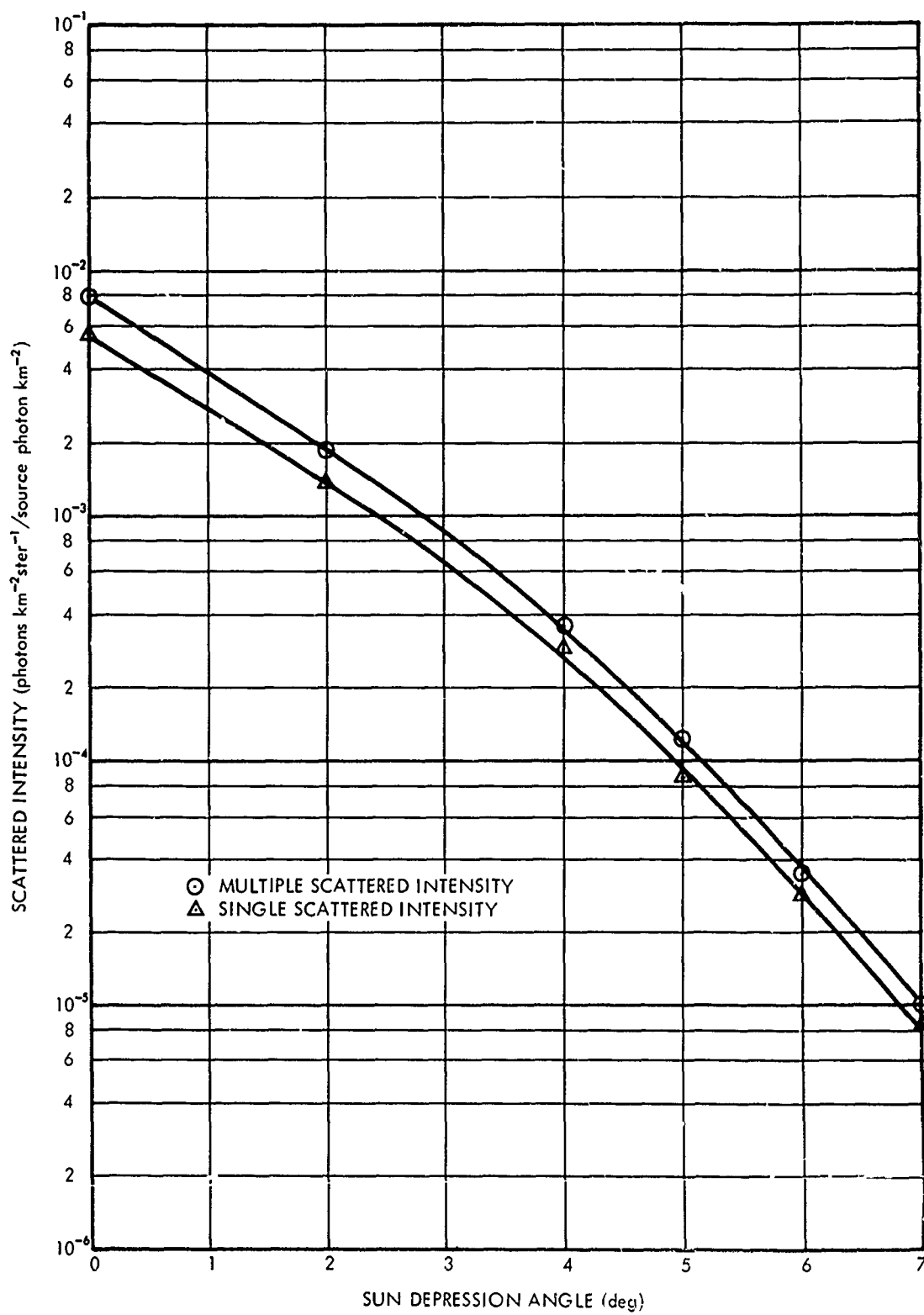


Fig. 12. Scattered Light Intensity at 20 Degrees Elevation versus Sun Depression Angle for Aerorol Profile C: 0.7μ Wavelength Light

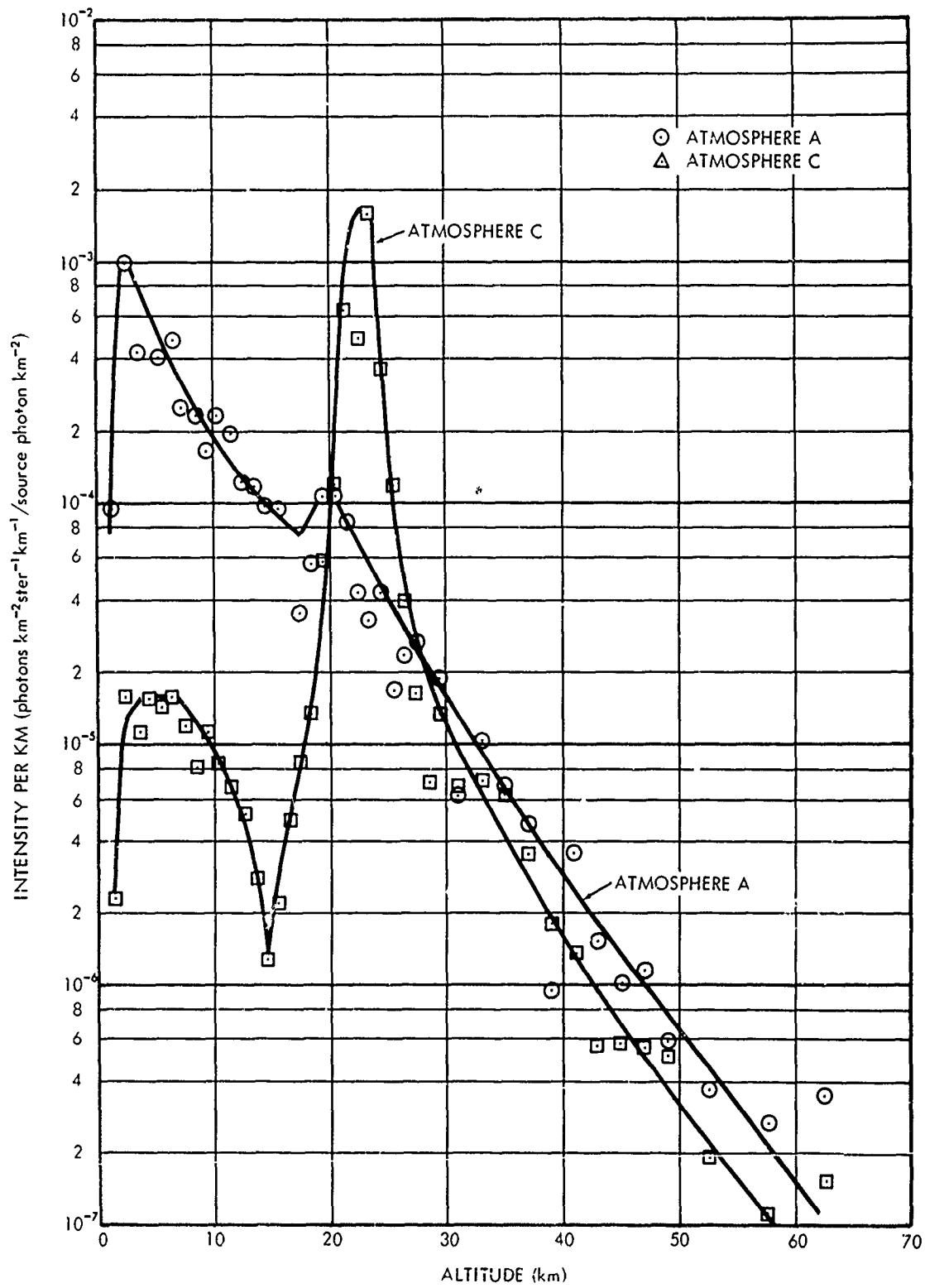


Fig. 13. Single Scattered Intensity for a Sun Depression Angle of 0° as a Function of Altitude in Atmospheres A and C: $\lambda = 0.7\mu$

REFERENCES

1. Collins, D. G., Atmospheric Path Radiance Calculations for a Model Atmosphere, Radiation Research Associates, Inc. Report RRA-M82 (AFCRL-68-0124), 13 March 1968.
2. Collins, D. G., Study of Polarization of Atmospheric Scattered Light Using Monte Carlo Methods, Radiation Research Associates, Inc. Report RRA-T86 (AFCRL-68-0310), 31 May 1968.
3. Wells, M. B., Monte Carlo Analysis of Searchlight Scattering Measurements, Radiation Research Associates, Inc. Report RRA-T87 (AFCRL-68-0311), 31 May 1968.
4. Collins, D. G. and Wells, M. B., Scattering and Reflectance of Light from Airborne Laser Systems, Radiation Research Associates, Inc. Report RRA-T88 (AFCRL-68-0479), 13 June 1968.
5. Collins, D. G. and Wells, M. B., Comparison of Atmospheric Path Radiance Calculations for Model Clear and Hazy Atmospheres, Radiation Research Associates, Inc. Report RRA-T89 (AFCRL-68-0480), 15 June 1968.
6. Wells, M. B., Collins, D. G., and Hopper, F. A., Contrast Transmission Data for Clear and Hazy Model Tropical Atmospheres, Radiation Research Associates, Inc. Report RRA-T92, Vols. I, II, and III (AFCRL-68-0660 (I, II, and III)), 1 December 1968.
7. Collins, D. G., Wells, M. B., and Fenn, R. W., Atmospheric Contrast Transmission Effects on Low Light Level TV Performance, CIRADS III Proceedings (U), Vol. II, AD394300, 15-17 October 1968 (C).
8. Chandrasekhar, S., Radiative Transfer, Dover Publications, Inc., New York, New York, 1960.
9. Coulson, K. L., Dave, J. V., and Sekera, Z., Tables Related to Radiation Emerging from a Planetary Atmosphere with Rayleigh Scattering, University of California Press, Berkeley and Los Angeles, 1960.
10. Collins, D. G. and Wells, M. B., Monte Carlo Codes for Study of Light Transport in the Atmosphere, Volumes I and II, Radiation Research Associates, Inc. Report ECOM-00240-F, August 1965.

11. Wells, M. B., Collins, D. G., and Cunningham, K., Light Transport in the Atmosphere, Volume I: Monte Carlo Studies, Radiation Research Associates, Inc. Report ECOM-00240-1, Vol. I, September 1966.
12. Cunningham, K., Wells, M. B. and Collins, D. G., Light Transport in the Atmosphere, Volume II: Machine Codes for Calculation of Aerosol Scattering and Absorption Coefficients, Radiation Research Associates, Inc. Report ECOM-00240-1, Vol. II, September 1966.
13. Carpenter, R. O., Scientific Report No. 1, Geophysical Research Directorate, Air Force Cambridge Research Center, Bedford, Massachusetts
14. Green, A. E. S., and Griggs, M., Applied Optics, Vol. 2, No. 6, p. 561 June 1963.
15. Burch, D. E., et al., Aeronutronic Division of Philco Corporation, Newport Beach, California, Reports U-3200, U-4367, U-3127, U-3030, U-3858, U-3972, U-2955, U-3201, and U-4132.
16. Skull, V. R., Wyatt, P. V., and Plass, G. N., Report No. SSD-TDR-62-127, Vol. III, Aeronutronic Division of Ford Motor Co., Newport Beach, California, 1963, AD 400 959.
17. Howard, J. N., Burch, D. E. and Williams, D., Sci. Rept. 1, GRD, AFCRL, The Ohio State University Research Foundation (Dec. 1954).
18. Elterman, L., Atmospheric Attenuation Model, 1964, in the Ultraviolet, Visible and Infrared Regions for Altitudes to 50 KM, Air Force Cambridge Research Laboratories Report AFCRL-64-740, September 1964
19. Elterman, L., An Atlas of Aerosol Attenuation and Extinction Profiles for the Troposphere and Stratosphere. Air Force Cambridge Research Laboratory Report, AFCRL-66-828, December 1966.
20. Wells, M. B. and Marshall, J. D., Monochromatic Light Intensities Above the Atmosphere Resulting from Atmospheric Scattering and Terrestrial Reflection, Radiation Research Associates, Inc. Report RRA-T85, 27 April 1968.

Unclassified

Security Classification

DOCUMENT CONTROL DATA - R & D

(Security classification of title, body of abstract and indexing annotation must be entered when the overall report is classified)

1. ORIGINATING ACTIVITY (Corporate author) Radiation Research Associates, Inc. 3550 Hulen Street Fort Worth, Texas 76107		2a. REPORT SECURITY CLASSIFICATION Unclassified
		2b. GROUP
3. REPORT TITLE FLASH, A MONTE CARLO PROCEDURE FOR USE IN CALCULATING LIGHT SCATTERING IN A SPHERICAL SHELL ATMOSPHERE		
4. DESCRIPTIVE NOTES (Type of report and inclusive dates) Scientific - Final (1 May 1967 - 31 January 1970)		Approved 10 April 1970
5. AUTHOR(S) (First name, middle initial, last name) Dave G. Collins Michael B. Wells		
6. REPORT DATE 31 January 1970	7a. TOTAL NO. OF PAGES 46	7b. NO. OF REFS 20
8a. CONTRACT OR GRANT NO. F19628-67-C-0298	8a. ORIGINATOR'S REPORT NUMBER(S) RRA-T704	
b. PROJECT NO. Task, Work Unit Nos. 7621-07-01		
c. DOD Element 62101F	9b. OTHER REPORT NO(S) (Any other numbers that may be assigned this report) AFCRL-70-0206	
d. DoD Subelement 681000		
10. DISTRIBUTION STATEMENT This document has been approved for public release and sale; its distribution is unlimited.		
11. SUPPLEMENTARY NOTES TECH, OTHER	12. SPONSORING MILITARY ACTIVITY Air Force Cambridge Research Laboratories (CROA) L. G. Hanscom Field Bedford, Massachusetts 01730	
13. ABSTRACT A program designated FLASH has been developed to provide a means to study the propagation of monochromatic radiation from a plane parallel source through a spherical shell atmosphere. A simple illustration of the backward Monte Carlo method utilized in the development of the FLASH program is discussed in order to show the advantage of the method. A brief description of the methods employed in the FLASH program is given to illustrate the application of the backward Monte Carlo treatment of light propagation through a spherical shell atmosphere. Several comparisons of FLASH generated data with data from other calculational methods are shown.		

DD FORM 1473
NOV 66

REPLACES DD FORM 1473, 1 JAN 64, WHICH IS OBSOLETE FOR ARMY USE.

Unclassified

Security Classification

14. KEY WORDS	LINK A		LINK B		LINK C	
	ROLE	WT	ROLE	WT	ROLE	WT
Monte Carlo Spherical Geometry Atmosphere Light Transport Twilight Scattering Sunlight Scattering Atmospheric Attenuation						